Saudi Dental Journal (2020) 32, 403–409

King Saud University

Saudi Dental Journal

www.ksu.edu.sa
www.sciencedirect.com

ORIGINAL ARTICLE

Identification of mandibular canal in cone beam computed tomography plane with different voxel sizes

Ameera Alabdulwahid, Wafa Alfaleh *

King Saud University, College of Dentistry, Riyadh, Saudi Arabia

Received 23 May 2019; revised 21 October 2019; accepted 23 October 2019
Available online 6 November 2019

KEYWORDS

Mandibular canal;
Voxel size;
CBCT;
Observers' agreement

Abstract *Introduction:* Identification of the mandibular canal (MC) is essential before any lower jaw surgical procedures. Understanding the anatomical variations of the MC is essential for preventing postoperative complications.

Objectives: We assessed the observer agreement for identifying the MC in cone-beam computed tomography (CBCT) images and to study the effect of changing the voxel size on such agreements.

Material and methods: We obtained images of mandibles from ten dry skulls using a water phantom with two voxels: 0.18 and 0.3 mm. The identification of the MC was made in five sites bilaterally in each mandible by two examiners.

Results: A total of 82 sites were included. Differences in measurements between images obtained with each scanning protocol and the reference images were calculated using descriptive statistics. There was an agreement between the two examiners in identifying the MC in CBCT images. No significant differences were found for identifying the MC when the voxel sizes were changed. There was a strong correlation coefficient between the two examiners for both voxel sizes ($p < 0.001$).

Conclusion: This study showed that voxel size, in the range from 0.18 to 0.3 mm, has no direct effect on the identification of the MC.

1. Introduction

The mandibular canal (MC) houses the inferior alveolar canal and blood vessels, and is considered as one of the most critical structures in the lower jaw. The detection of the MC has the utmost importance before planning surgical procedures that involve the posterior area of the mandible, such as osteotomies, bone harvesting procedures, dental implant placement, and surgical removal of third molars (Angelopoulos et al., 2008). Understanding the anatomical variations of the MC is

* Corresponding author at: Department of Oral Medicine and Diagnostic Science, Division of Oral &Maxillofacial Radiology, College of Dentistry, King Saud University, P.O. Box 5967, Riyadh 11432, Saudi Arabia.
E-mail addresses: ameera@ksu.edu.sa (A. Alabdulwahid), wafaalfaleh2000@gmail.com (W. Alfaleh).

Peer review under responsibility of King Saud University.

Production and hosting by Elsevier

https://doi.org/10.1016/j.sdentj.2019.10.009

essential for avoiding a probable sensory disorder, hemorrhagic complications, and even anesthesia failures (Lew and Townsen, 2006). Therefore, variations in the pathway of the MC, as it runs through the lower jaw, must be recognized by clinicians.

Different radiographic modalities have been used to assess the course of the MC (Angelopoulos et al., 2008; Lindh and Petersson, 1989). Cone-beam computed tomography (CBCT) is commonly used in dental and radiological practices (Angelopoulos et al., 2008; Scarfe et al., 2006). It has an advantage, in comparison to conventional 2D images, in the elimination of superimposition of adjacent structures. The quality of the image produced by CBCT, and its ability to display anatomically detailed of structures as well as any pathological disorder, is affected by a numerous variables among them the scanning unit, size of the field to be viewed (FOV), object to being scanned, exposure time, and voxel size (Kamburoglu et al., 2011). The voxel size variable within the CBCT machine producing variable protocol depending on the purpose of the image. Generally, the resolution of the images is improved when smaller voxel sizes are used (Stratemann et al., 2008). In 2007, Levine et al. studied the location of the MC in the reformatted cross-sectional plane of the lower jaw; their results showed good to excellent intra-examiner agreement between the two examiners.

In 2009, Lofthag-Hansen et al. performed a study to evaluate observers' agreement and discernibility of the MC and crest of the alveolar ridge using CBCT. They found that there was difficulty in identifying the MC in predetermined cross-sectional images. However, approaching more reformatted orthogonal planes improved identification with better visualization of the canal (Lofthag-Hansen et al., 2009). However, little is known about the effects of voxel size in the identification of MC in the CBCT reformatted plane. Therefore, this study aimed to reveal the observer agreement in identifying the MC and to explore the influence of voxel size changes on the observer agreement.

2. Materials and methods

2.1. Selection of specimens

This investigational study was approved by the Human Ethics Committee of the Institutional Review Board (Approval Number PR 0004).

Five natural dried skulls of humans were borrowed from the Anatomy Department in the College of Medicine, King Saud University, as well as mandibles of five dry skulls owned by the Radiology Department at College of Dentistry, King Saud University. A total of ten dry human skulls were included in this research.

The mandibles were free from fractures and metallic restorations to avoid possible scattering and artifact formation. Five measurement sites were selected on each side of the mandible, located at the region between lower premolars, between the second premolar and first molar, between first and second molar, between the second and third lower molar and distal to the third molar. A total of 100 sites on the ten dry mandibles were included.

As has been described in previous publications by Al-Ekrish and Ekram (2011), to identify each measurement site, a vertical line was drawn perpendicular to the base of the mandible, delineating its bony contours: the buccal cortex, alveolar bone crest, and lingual cortex. On each of the three surfaces, a 1-mm mark was made on the line using permanent ink. To make sure the position and orientation of each sample site would not be changed between different protocols, as well as the direction of measurements, gutta-percha (GP) markers were glued onto the crest of the ridge as well as the corresponding buccal and

Fig. 1 Photograph of the dry mandible showing the location of GP markers.

lingual surfaces of the mandible and to allow for identification of each site on the different orthogonal planes (Fig. 1).

2.2. Image acquisition

As described by Yamany (2011), the mandibles were immersed in a thin, clear plastic container. Soft tissue compensation obtained by using water. The amount of water was measured to be the same with all mandibles ensuring that the whole mandibles were covered with water. Each mandible was scanned twice for each protocol without changing the position of the mandible within the container to ensure that the amount of water in the container was the same during the scanning of all mandibles, a plastic syringe was used to inject water into the MC through the mandibular foramen to avoid air bubbles entrapment.

CBCT base images were obtained with Carestream® CS 9300 CBCT equipped with a digital receptor, operating with 70 kVp and 4 mA. The mandible was positioned on the unit and scanned two times, according to the voxel size selected: voxel 0.18 mm and voxel 0.3 mm. (FOV, 10 cm height and 5 cm diameter; acquisition time, 6.2 s).

2.3. Reference images

The mandibles were imaged without soft tissue compensation. For localization of the canal, a 0.41 mm round brass wire was placed in the MC starting from the mandibular foramen. The wire was used to assist in locating the canal and confirm the correct identification of the canal. Reformatted images were obtained with the same method mentioned above. Both examiners were calibrated until they reached consensus on the agreed measured distance from the reference GP placed at the crest of the alveolar ridge to the outer roof of MC. These measurements were used as a gold standard measurement for comparison of the two different protocols.

2.4. Image reconstruction and sample site preparation

The images scanned were saved as DICOM (digital imaging and communications in medicine) format and transferred to another computer equipped with 3D image reformatting software, the OnDemand3D™ software, (OnDemand Software, version 1.0, Cybermed Inc., Seoul, South Korea) (Al-Ekrish et al., 2016).

The first author (A.A.) with five years of experience in CBCT reformatting prepared all the datasets to obtain transverse cross-sectional images of the requested sample sites. Default position and orientation of the orthogonal sectional planes were consistent in all of the samples of the two protocols of CBCT datasets. Thus, standardization of the site and orientation of the reformatted sample sites was achieved between two protocols.

The 3D module was used to obtain the reformatted orthogonal plane (cross-sections) which is perpendicular to the mandible corresponding to the sites marked by the GP markers, the slices selected for visualization of the canal and subsequent measurements by the observers were those that include all three markers (Fig. 2), the identification information was masked to avoid recognition of the protocol. Each reformatted dataset saved as a bookmark within the master database of the reformatting software program. The examiners then accessed the saved bookmarks to record the measurements. The examiners were able to view the images in all the orthogonal planes and scroll through the dataset for better visualization of the IAC. However, to record the measurements, the examiners had to revert to the bookmarked sample site.

2.5. Image interpretation

Interpretation of the chosen sites as described by Al-Ekrish et al. in 2016, the sagittal coordinate was aligned parallel to the mandible in the axial plane. The coronal coordinate was aligned perpendicular to the mandible at each selected site. In the cross-sectional and parasagittal views, these coordinates were adjusted to make sure that all three GP markers were demonstrated on the selected image (Fig. 2A). The examiners were oral and maxillofacial radiologists (A.A. and W.F.) with several years of experience in CBCT interpretation. They recorded the measurements using the ruler tool under dim light. The observers were allowed to magnify the images for optimum clarity, as well as adjust the contrast and brightness of the images. Each examiner measured the distance by drawing a line joining the outer surface of reference GP located on the crest of the alveolar ridge to the outer roof of the canal (Fig. 2B). The height measurement of the ridge was recorded on the sample site along the line representing the oblique sagittal plane.

For assessment of reliability, the first examiner repeated all of the measurements for both protocols one month later.

2.6. Statistical analysis

Statistical analysis was done using SPSS for Windows (v. 22; SPSS Inc., Chicago, IL), the differences in measurements between images with each scanning protocol and the reference images were calculated using descriptive statistics. The mean of the absolute values of the differences was calculated for each protocol for the overall measurements.

Intra- and inter-examiner reliability were assessed with correlation testing and calculation of Cronbach's Alpha, which was used in the same respect in order to confirm the results of the correlation testing.

To test the statistical significance of the difference between the means of the measurements obtained from each protocol and those obtained from the reference images a paired *t*-test was used. An independent *t*-test was used to test the difference between the two examiners for each protocol. The means of the absolute differences between the two protocols were then tested for significance using the independent *t*-test.

Results with a p-value < 0.05 were considered to be statistically significant.

3. Results

Eighty-two mandibular sites were included in the study, while 18 sites were excluded for either the wire did not reach the premolar area, or it ran out of the MC. Thus, the total obtained number was 164 CBCT dataset; 82 for each voxel size as well as for the reference images at α level of significance 0.05 with power $(1\text{-}\beta) = 0.81$ and effect size 0.8 or 8% the sample size should be at least eight sites per tooth.

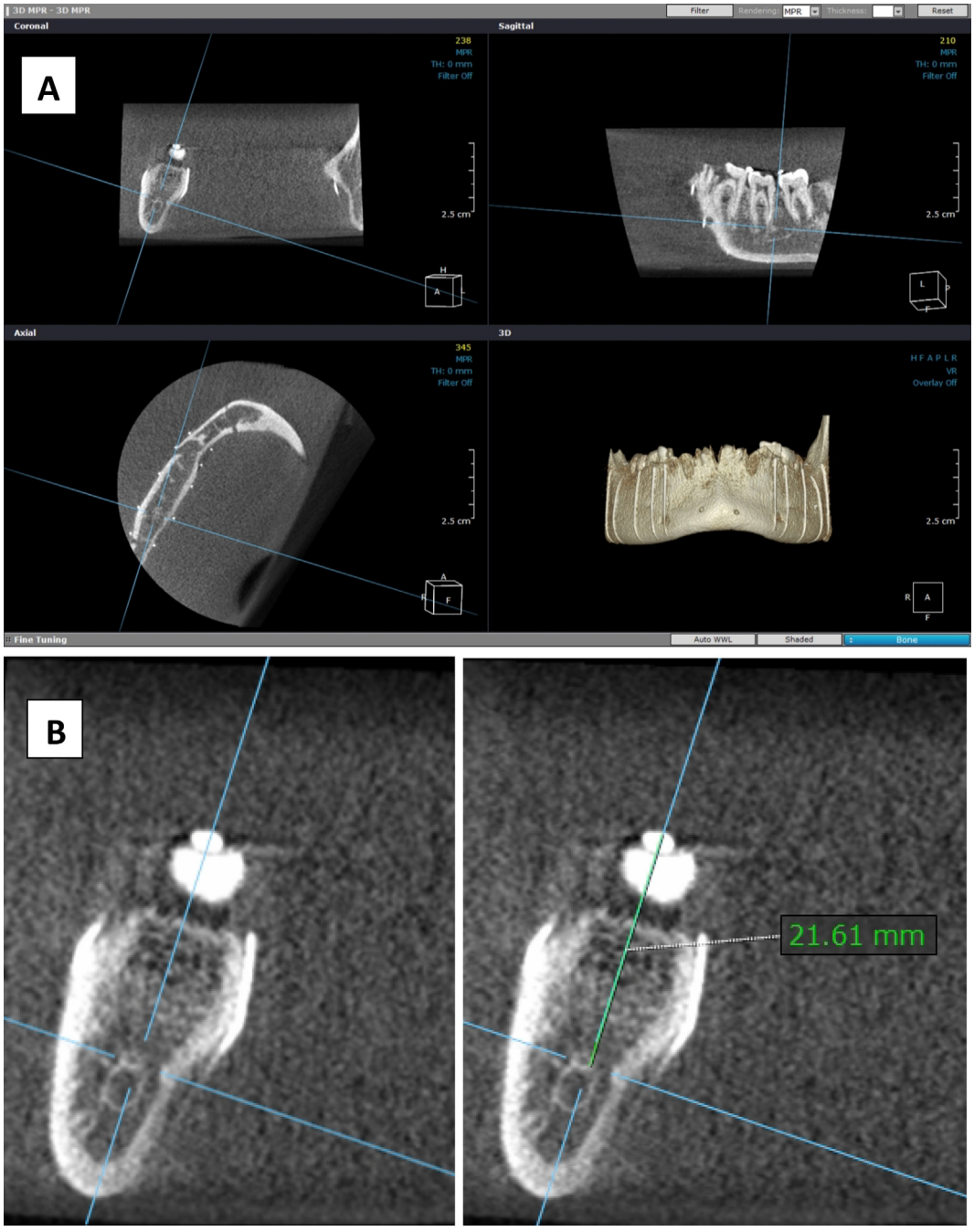

Fig. 2 (A) Orthogonal plans demonstrate the alignment of the coordinates at measurement site showing three GP makers. (B) Transverse cross sectional image of area showing the direction of measurement.

3.1. Reliability testing

3.1.1. Intra-examiner reliability

The first examiner (A) recorded all measurements twice. The measurements recorded by the first examiner were used to calculate the intra-examiner reliability for both protocols. The Pearson Correlation coefficients for voxel size 0.18 mm and voxel size 0.3 mm were 0.95 and 0.91, respectively, with a p-value < 0.001. This indicates a highly significant correlation between the two readings by the first examiner for both voxel sizes. Cronbach's Alpha results for voxel sizes 0.18 mm and 0.3 mm were 0.94 and 0.90, respectively. These findings indicated high intra-examiner reliability.

3.1.2. Inter-examiner reliability

For voxel 0.18 mm, the Pearson correlation coefficient was 0.95, which means that there was a strong significant correlation between the first examiner (A) and the second examiner (B) with p-value < 0.001. For voxel 0.3 mm, the Pearson correlation coefficient was 0.87, which means that there was a strong significant correlation between Examiner A and B with (p-value < 0.001).

3.2. Measurement errors

The measurement error was analyzed by subtracting the value obtained from the reference images from the value obtained from the images using (0.18 and 0.3 mm voxel size). The mean of measurements error for 0.18 mm voxel size as compared to the reference images measurements for the examiner (A) were −1.63 mm less than the reference images and 0.87 mm more than the reference images. While for voxel size 0.3 mm, it was −1.68 mm less than the reference images and 1.76 mm more than the reference images. For the second examiner, the mean of measurement error for 0.18 mm voxel size, as compared to the reference images measurements, was −1.51 less than the reference images and 0.79 mm more than the reference images. While for voxel size, 0.3 mm was −1.77 mm less than the reference images and 1.49 mm more than the reference images, which indicates that in 0.3 mm voxel size, the measurement was *overestimated* than 0.18 mm voxel for both examiners. Fig. 3 illustrates the Percentage of absolute errors for both protocols (0.18 and 0.3 mm) for both examiners A and B.

3.3. Comparison between 0.18 mm and 0.3 mm measurements

Paired *t*-test showed no significant differences between the radiographic images of each protocol compared to the reference images for each examiner with a *p*-value < 0.05 (Table 1). An independent *t*-test was used to test the difference between the two examiners for each protocol, and no significant difference was found with *p*-value < 0.05 (Table 2).

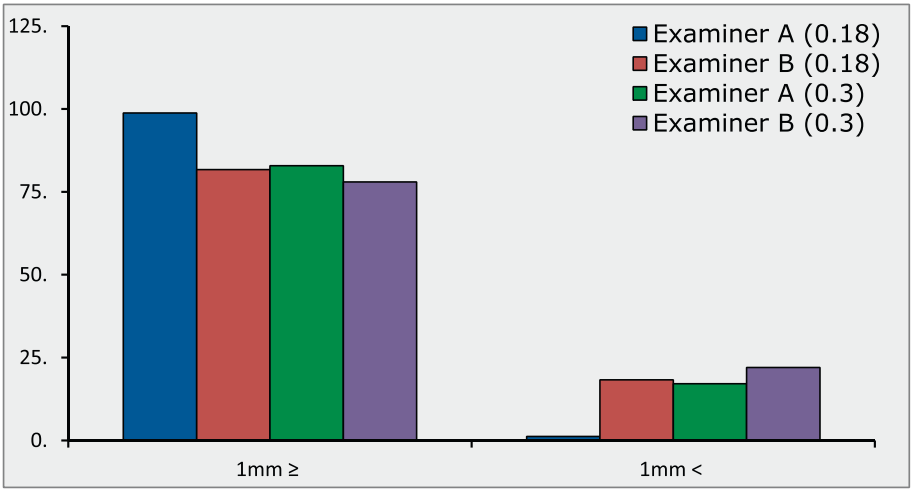

Fig. 3 Percentage (%) of absolute errors for both protocols (0.18 and 0.3 mm) for examiners A and B.

Table 1 Descriptive statistics of both examiners between (0.18), (0.3) voxel size and the reference images with p value < 0.05.

Examiner A	Voxel size (mm)	N	Mean (mm)	Standard Deviation	Standard Error (mm)	P-value
	(0.18)	82	17.48	5.16	0.57	0.203
	Wire		17.43	5.19	0.57	
	(0.30)		17.52	5.12	0.56	0.28
	Wire		17.43	5.19	0.57	
	(0.18)		17.48	5.16	0.57	0.664
	(0.30)		17.52	5.12	0.56	
Examiner B	(0.18)	82	17.59	5.17	0.57	0.071
	Wire		17.43	5.19	0.57	
	(0.30)		17.59	5.03	0.56	0.094
	Wire		17.43	5.19	0.57	
	(0.18)		17.59	5.17	0.57	0.988
	(0.30)		17.59	5.03	0.56	

Table 2 The mean and standard deviation for both examiner A and B for each protocol.

Voxel Size (mm)	Examiner	N	Mean (mm)	Standard Deviation	Standard Error Mean (mm)	P-value
(0.18)	A	82	17.48	5.16	0.57	0.887
	B		17.59	5.17	0.57	
(0.30)	A		17.52	5.12	0.56	0.922
	B		17.59	5.03	0.56	

4. Discussion

Various imaging modalities are used to identify the MC; the optimal technique would permit identification and measurement of the MC in relation to the alveolar crest within 1 mm. Two-dimensional radiographs provide limited information related to the location of the MC. Multi-Detector CT (MDCT) has been used before the introduction of CBCT to determine the location of the MC. This canal has been demonstrated clearly in cross-sectional CT images than a conventional 2D image, but it exposed patients to high radiation dose. CBCT imparts a lower radiation dose than MDCT. Therefore, it alleviates concerns about radiation doses. This justifies the use of CBCT in this study to identify the location of MC in the mandible.

The appearance of the final produced image affected by many factors. The size of the voxel affects the noise in produced sections of an image: the smaller the voxel size, the higher the noise; hence, the spatial resolution will be improved (Al-Rawi et al., 2010).

The MC can be identified easily if its outline is corticated. If the canal is non corticated, it will be difficult to correctly identify the canal from the adjacent bone marrow spaces (Wadu et al., 1997).

In Carter (1971), compared the radiographic appearance of the MC with the actual situation revealed in the dissection. The radiopaque lines surrounding the MC showed marked variation between individuals in terms of their continuity. In some cases, the MC could not be distinguished at all. Therefore, a wire was used in this study as a reference image to precisely identify the location of MC. In this study, we found that the corticated MC was easier to be identified than the noncorticated MC. This finding is supported by the results obtained by Angelopoulos et al. (2008) and Wadu et al. (1997).

In a study by Lofthag-Hansen et al. (2009), multiple observers assessed the discernibility and the location of the MC in relation to the crest of the alveolar ridge two times by visually determining if the structures could be seen clearly, if they were probably visible, or if they were invisible in a predetermined cross-sectional image. If the decision was not "clearly visible," or if the anatomic structures were difficult to identify, the observers assessed other cross-sectional, axial, and/or sagittal images in the volume. The observers found it difficult to identify the MC with only one single cross-sectional image. Their accuracy was improved by using multiple images in different plans (Lofthag-Hansen et al., 2009), which is the same as our finding. This explains the high agreement between the two observers for identifying the MC. Although Waltrick et al. (2013) reported that transverse images were adequate for visualization of the MC, this contradicts the findings reported in this study where it was challenging to identify the MC depending only on transverse images. Therefore, other planes were used to accurately identify the canal (Waltrick et al., 2013).

Hideyuki Tanimoto (2009) found that choosing a small voxel size without changing the radiation dose increased the resolution. Personal communication with Kodak Company confirmed that, with the Carestream® CS 9300 CBCT machine, the use of small voxel size did not increase the Dose Area Product (DAP) since both voxel sizes use the same number of projections with the same number of x-ray pulses, but not the same number of slices. We found that both voxel sizes had the same Dose Area Product (DAP), which was 183 $mGy.cm^2$. When we used a smaller voxel size (0.18 mm) DAP wasn't increased. However, the resolution of the images was increased compared to the 0.3 mm voxel size Further research is recommended to evaluate the DAP in both protocols.

The present study's finding of a lack of significant difference in the visibility of the MC in images using 0.18 mm and 0.3 mm voxel sizes are supported by the findings of Oliveria-Santos et al. (2011), who concluded that 0.3 mm voxel size can be recommended for identification of the MC. The lack of difference in visibility of the canal found in the present study was, in spite of the fact that the examiners were more confident in identification of the MC on images using the 0.18 mm voxel sizes, which is similar to the findings reported by previous investigators (Damstra et al., 2010; Kamburoglu et al., 2010; Torres et al., 2012; de-Azevedo et al., 2013; Neves et al., 2012; Liedke et al., 2009; Ozer, 2011; Melo et al., 2010; Librizzi et al., 2011; Sun et al., 2011; Dalili et al., 2012; da Silveira et al., 2013).

In this study, both inter- and intra-examiner agreements were high, in agreement with Levine et al. (2007). This agreement could be attributed to the use of reference points before imaging the mandibles, the use of interactive cross-sectional images—other than the predetermined cross-sectional or static images—and familiarity with the software.

One key study limitation warrants consideration. The dry mandibles that were selected for this study were free from any metallic objects; however, this does not simulate "real world" clinical situations. Therefore, it is not clear if the metallic artifact could lead to image degradation and affect the localization of the MC.

5. Conclusion

Using a small voxel size produces images with a high spatial resolution but may expose patients to more radiation. This study showed that voxel size, in the range from 0.18 to 0.3 mm, had no direct effect on the identification of the MC.

Declaration of Competing Interest

The authors of this manuscript have no conflict of interest ro declare.

References

Al-Ekrish, A.A., Ekram, M., 2011. A comparative study of the accuracy and reliability of multidetector computed tomography and cone-beam computed tomography in the assessment of dental implant site dimensions. Dentomaxillofac Radiol. 40 (2), 67–75.

Al-Ekrish, A.A., Al-Shawaf, R., Schullian, P., et al, 2016. Validity of linear measurement of the jaws using ultralow-dose MDCT and the iterative techniques of ASIR and MBIR. Int. J. CARS Oct (11), 1791–1801.

Al-Rawi, B., Hassan, B., Vandenberge, B., Jacobs, R., 2010. Accuracy assessment of three-dimensional surface reconstructions of teeth from cone-beam computed tomography scans. J. Oral Rehabil. 37 (5), 352–358.

Angelopoulos, C., Thomas, S.L., Hechler, S., Parissis, N., Hlavacek, M., 2008. Comparison between digital panoramic radiography and

cone-beam computed tomography for the identification of the mandibular canal as part of presurgical dental implant assessment. J. Oral Maxillofac Surg. 66 (10), 2130–2135.

Carter, K., 1971. The intramandibular course of the inferior alveolar nerve. J. Anat. 3 (108), 433–440.

da Silveira, P.F., Vizzotto, M.B., Liedke, G.S., da Silveira, H.L., Montagner, F., da Silveira, H.E., 2013. Detection of vertical root fractures by conventional radiographic examination and cone-beam computed tomography - an in vitro analysis. Dent. Trauma 29 (1), 41–46.

Dalili, Z., Taramsari, M., Mousavi Mehr, S.Z., Salamat, F., 2012. Diagnostic value of two modes of cone-beam computed tomography in evaluation of simulated external root resorption: an in vitro study. Imaging Sci. Dent. 42 (1), 19–24.

Damstra, J., Fourie, Z., Huddleston Slater, J.J., Ren, Y., 2010. Accuracy of linear measurements from cone-beam computed tomography-derived surface models of different voxel sizes. Am. J. Orthod. Dentofac. Orthop. 137 (1). 16 e11–16.

de-Azevedo-Vaz, S.L., Vasconcelos, K.D.F., Neves, F.S., Melo, S.L. S., Campos, P.S.F., Haiter-Neto, F., 2013. Detection of peri-implant fenestration and dehiscence with the use of two scan modes and the smallest voxel sizes of a cone-beam computed tomography device. Oral Surg. Oral. Med. Oral Pathol. Oral Radiol. 115 (1), 121–127.

Hideyuki Tanimoto, Y.A., 2009. The effect of voxel size on image reconstruction in cone-beam computed tomography. Oral Radiol. 25, 149–153.

Kamburoglu, K., Murat, S., Kolsuz, E., Kurt, H., Yuksel, S., Paksoy, C., 2011. Comparative assessment of subjective image quality of cross-sectional cone-beam computed tomography scans. J. Oral Sci. 53 (4), 501–508.

Kamburoğlu, K., Murat, S., Yüksel, S.P., Cebeci, A.R.İ., Paksoy, C. S., 2010. Occlusal caries detection by using a cone-beam CT with different voxel resolutions and a digital intraoral sensor. Oral Surg. Oral Med. Oral Pathol. Oral Radiol. Endod. 109 (5), e63–e69.

Levine, M.H., Goddard, A.L., Dodson, T.B., 2007. Inferior alveolar nerve canal position: a clinical and radiographic study. J. Oral Maxillofac. Surg. 65 (3), 470–474.

Lew, K., Townsen, G., 2006. Failure to obtain adequate anaesthesia associated with a bifid mandibular canal: a case report. Aust. Dent. J. 51 (1), 86–90.

Librizzi, Z.T., Tadinada, A.S., Valiyaparambil, J.V., Lurie, A.G., Mallya, S.M., 2011. Cone-beam computed tomography to detect erosions of the temporomandibular joint: Effect of field of view and voxel size on diagnostic efficacy and effective dose. Am. J. Orthod. Dentofac. Orthop. 140 (1), e25–30.

Liedke, G.S., da Silveira, H.E., da Silveira, H.L., Dutra, V., de Figueiredo, J.A., 2009. Influence of voxel size in the diagnostic ability of cone-beam tomography to evaluate simulated external root resorption. J. Endod. 35 (2), 233–235.

Lindh, C., Petersson, A., 1989. Radiologic examination for location of the mandibular canal: a comparison between panoramic radiography and conventional tomography. Int. J. Oral Maxillofac. Implants 4 (3), 249–253.

Lofthag-Hansen, S., Grondahl, K., Ekestubbe, A., 2009. Cone-beam CT for preoperative implant planning in the posterior mandible: visibility of anatomic landmarks. Clin. Implant. Dent. Relat. Res. 11 (3), 246–255.

Melo, S.L.S., Bortoluzzi, E.A., Abreu Jr, M., Corrêa, L.R., Corrêa, M., 2010. Diagnostic ability of a cone-beam computed tomography scan to assess longitudinal root fractures in prosthetically treated teeth. J. Endod. 36 (11), 1879–1882.

Neves, F., Vasconcelos, T., Vaz, S., Freitas, D., Haiter-Neto, F., 2012. Evaluation of reconstructed images with different voxel sizes of acquisition in the diagnosis of simulated external root resorption using cone-beam computed tomography. Int. Endod. J. 45 (3), 234–239.

Oliveira-Santos, C., Capelozza, A.L., Dezzoti, M.S., Fischer, C.M., Poleti, M.L., Rubira-Bullen, I.R., 2011. Visibility of the mandibular canal on CBCT cross-sectional images. J. Appl. Oral Sci.: Revista FOB 19 (3), 240–243.

Ozer, S.Y., 2011. Detection of vertical root fractures by using cone-beam computed tomography with variable voxel sizes in an in vitro model. J. Endod. 37 (1), 75–79.

Scarfe, W.C., Farman, A.G., Sukovic, P., 2006. Clinical applications of cone-beam computed tomography in dental practice. J. Can. Dent. Assoc. 72 (1), 75–80.

Stratemann, S.A., Huang, J.C., Maki, K., Miller, A.J., Hatcher, D.C., 2008. Comparison of cone-beam computed tomography imaging with physical measures. Dent. Maxillo Radiol. 37 (2), 80–93.

Sun, Z., Smith, T., Kortam, S., Kim, D.G., Tee, B.C., Fields, H., 2011. Effect of bone thickness on alveolar bone-height measurements from cone-beam computed tomography images. Am J Orthod Dentofac Orthop 139 (2). e117–127.

Torres, M.G., Campos, P.S., Segundo, N.P., Navarro, M., Crusoe-Rebello, I., 2012. Accuracy of linear measurements in cone-beam computed tomography with different voxel sizes. Implant. Dent. 21 (2), 150–155.

Wadu, S.G., Penhall, B., Townsend, G.C., 1997. Morphological variability of the human inferior alveolar nerve. Clin. Anat. (New York, NY) 10 (2), 82–87.

Waltrick, K.B., de Abreu Junior, M.J., Correa, M., Zastrow, M.D., D'Avila Dutra, V., 2013. Accuracy of linear measurements and visibility of the mandibular canal of cone-beam computed tomography images with different voxel sizes: an in vitro study. J. Periodontol. 84 (1), 68–77.

Yamany, I, 2011. A Comparative Analysis of Different Fields of View in Cone Beam Computed Tomography Imaging to Identify the Inferior Alveolar Nerve Canal. Master's Theses. Paper 131. http://digitalcommons.uconn.edu/gs_theses/131.